



HAL
open science

Coercivity tuning in Co/Pd multilayer based bit patterned media

O Hellwig, Thomas Hauet, T Thomson, E Dobisz, D. Risner-Jamtgaard, D Yaney, B. D. Terris, Eric E. Fullerton

► **To cite this version:**

O Hellwig, Thomas Hauet, T Thomson, E Dobisz, D. Risner-Jamtgaard, et al.. Coercivity tuning in Co/Pd multilayer based bit patterned media. Applied Physics Letters, 2009, 10.1063/1.3271679 . hal-01345323

HAL Id: hal-01345323

<https://hal.science/hal-01345323>

Submitted on 13 Jul 2016

HAL is a multi-disciplinary open access archive for the deposit and dissemination of scientific research documents, whether they are published or not. The documents may come from teaching and research institutions in France or abroad, or from public or private research centers.

L'archive ouverte pluridisciplinaire **HAL**, est destinée au dépôt et à la diffusion de documents scientifiques de niveau recherche, publiés ou non, émanant des établissements d'enseignement et de recherche français ou étrangers, des laboratoires publics ou privés.

Coercivity tuning in Co/Pd multilayer based bit patterned media

O. Hellwig,^{1,a)} T. Hauet,¹ T. Thomson,¹ E. Dobisz,¹ J. D. Risner-Jamtgaard,¹ D. Yaney,¹ B. D. Terris,¹ and E. E. Fullerton²

¹San Jose Research Center, Hitachi Global Storage Technologies, 3403 Yerba Buena Rd., San Jose, California 95135, USA

²Center for Magnetic Recording Research, University of California at San Diego, La Jolla, California 92093-0401, USA

(Received 19 September 2009; accepted 10 November 2009; published online 8 December 2009)

In order to adjust the reversal field of high anisotropy $[\text{Co}(2.8 \text{ \AA})/\text{Pd}(9 \text{ \AA})]_8$ bit patterned media (BPM), one may increase the individual Co thickness to change the overall anisotropy or alternatively combine the high anisotropy multilayer with a lower anisotropy material, thus creating a heterogeneous laminated system. In the current study, we find that $[\text{Co}/\text{Pd}]_8\text{-}[\text{Co}/\text{Ni}]_N$ hard-soft laminated BPM allows tuning the coercivity while maintaining a narrow normalized switching field distribution (σ_{SFD}/H_C), whereas homogeneous structures with increased individual Co thickness show a more pronounced increase in σ_{SFD}/H_C . Possible reasons for the different behavior, such as changes in strain and texture, are discussed. © 2009 American Institute of Physics. [doi:10.1063/1.3271679]

Magnetron sputtered $[\text{Co}/\text{Pd}]$ and $[\text{Co}/\text{Pt}]$ multilayers (ML) are model material systems for bit patterned media (BPM) due to their controllable magnetic properties.¹⁻³ Deposition parameters, such as individual Co and Pd layer thicknesses, number of repeats, sputter pressure, and temperature allow good control over magnetic properties including anisotropy, saturation magnetization, coercivity, and magnetic microstructure.^{4,5} One crucial issue for the implementation of BPM is to control the switching field and the switching field distribution (SFD) in order to ensure addressability of the predefined bits without overwriting adjacent down- or cross-track bits.^{2,6,7}

Here we use composite $[\text{Co}/\text{Pd}]/[\text{Co}/\text{Ni}]$ MLs for tuning the coercivity (H_C) and the SFD (σ_{SFD}) in BPM. The samples were fabricated at room temperature by dc magnetron sputtering onto prepatterned substrates at 3 mTorr Ar pressure. Using a Ta(15 Å)/Pd(30 Å) seed layer system we obtain (111)-textured MLs with a mosaic spread of 7° full width at half maximum (FWHM). In Fig. 1(a) we present an aberration corrected, high angle annular dark field (HAADF) scanning transmission electron microscopy (STEM) image of a Co(4 Å)/Pd(8 Å) ML structure. These images show that the Co layers are two and the Pd layers three to four atomic rows thick (in agreement with the deposition parameters) with an interface roughness of one monolayer or below, thus providing high interfacial anisotropy.

Example BPM structures are shown in Figs. 1(c)–1(e). Figure 1(c) is a $[\text{Co}(2.8 \text{ \AA})/\text{Pd}(9 \text{ \AA})]_8$ ML structure deposited onto prepatterned Si substrates with a 35 nm pitch. The bright field transmission electron microscopy (TEM) image shows trapezoidal-shaped prepatterned Si pillars with the magnetic ML films deposited on top of the islands and in the trenches between the pillars.⁸ For well-defined multilayers the prepatterned pillars need to have flat tops, sharp corners, and steep sidewalls. Energy filtered TEM (EFTEM) images for a thicker ML structure are shown in Figs. 1(d) and 1(e) and demonstrate well-defined layering on top of the pillars.

The ML structures are deposited using a con-focal sputter up geometry with the targets tilted and arranged in a circle around a center target (Pd) as illustrated in Fig. 1(b). The substrate, which rotates during deposition at 3 Hz, is at the focal point of the targets. With the Co target being tilted we obtain relatively more Co deposition onto the sidewalls than in the trenches, while for the center Pd target more material is deposited in the trenches and less on the sidewalls [Figs. 1(d) and 1(e)]. After depositing the Pd cap layer we take the samples out of the vacuum process chamber, which leads to oxidation of the Co-rich sidewalls, thus helping to magnetically decouple the ML islands from the Pd-rich trench material.⁹

Anisotropy field H_K and ML-averaged saturation magnetization M_S versus individual Co layer thickness are summa-

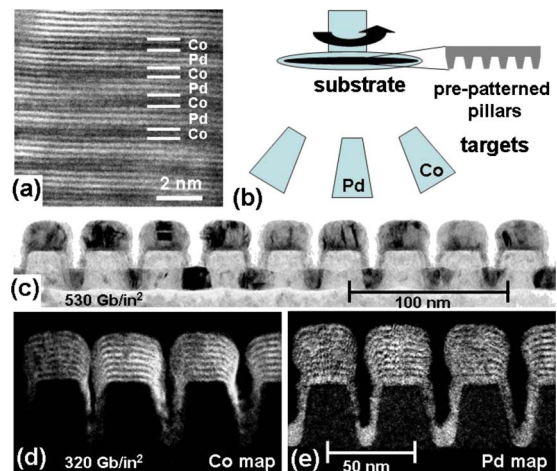


FIG. 1. (Color online) BPM fabricated by ML deposition onto prepatterned Si substrates: (a) Aberration corrected, HAADF STEM image of a Co(4 Å)/Pd(8 Å) ML. (b) Illustration of the con-focal sputter up geometry used for BPM fabrication. (c) Bright field TEM cross-sectional image of a row of islands with 35 nm pitch (530 Gb/in²) and a Ta(15 Å)/Pd(30 Å)/ $[\text{Co}(2.8 \text{ \AA})/\text{Pd}(9 \text{ \AA})]_8/\text{Pd}(11 \text{ \AA})$ ML. (d) and (e) are cross-sectional EFTEM elemental maps of a row of islands with 45 nm pitch (320 Gb/in²). For the films in (d) and (e) the ML period was increased to $[\text{Co}(17 \text{ \AA})/\text{Pd}(17 \text{ \AA})]_8$ in order to spatially resolve the layering.

^{a)}Electronic mail: olav.hellwig@hitachigst.com.

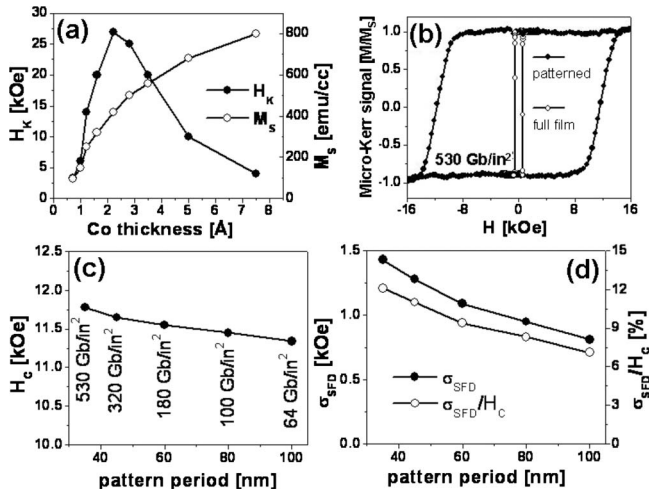


FIG. 2. BPM fabricated by ML deposition onto prepatterned substrates: (a) Anisotropy field H_K and ML-averaged saturation magnetization M_S vs individual Co layer thickness for $[\text{Co}(t)\text{Pd}(9 \text{ \AA})]_8$ MLs. (b) Microspot PMOKE hysteresis loop of the full film ML and from an array of islands at 530 Gb/in^2 areal density. (c) Coercivity (H_C) vs pattern period for a $[\text{Co}(2.8 \text{ \AA})/\text{Pd}(9 \text{ \AA})]_8$ ML film. (d) Absolute SFD (σ_{SFD}) and normalized SFD (σ_{SFD}/H_C) vs pattern period for the same ML film.

ized in Fig. 2(a) for $[\text{Co}(t)\text{Pd}(9)]_8$ ML structures. We find the highest out-of-plane anisotropy ($H_K=27 \text{ kOe}$, $H_{K,\text{eff}}=H_K-4\pi M_S=21 \text{ kOe}$) for a Co thickness of $2.5\text{--}3 \text{ \AA}$ and a Pd thickness of $8\text{--}10 \text{ \AA}$.¹⁰ Depositing such high anisotropy MLs with Co(2.8 \AA) on pre-patterned substrates we achieve $H_C=11\text{--}12 \text{ kOe}$, while for a continuous film we obtain $H_C=500 \text{ Oe}$. This is shown in Fig. 2(b) as measured by micro-focused polar magneto optic Kerr effect (PMOKE).^{1,2} The full film reversal is governed by nucleation and domain wall motion, while the isolated ML islands on the pillars reverse independently.^{1,9} The reversal field for small islands is significantly less than the effective anisotropy field $H_{K,\text{eff}}=21 \text{ kOe}$ due to thermal activation, nonuniform reversal modes and imperfections in the MLs, such as defects and misaligned grains, all of which act to lower H_C .

The loop from the patterned array in Fig. 2(b) shows no trench reversal at low fields,^{2,8,11} indicating that the amount of magnetic trench material is small [Fig. 1(d)]. In Figs. 2(c) and 2(d) we present the island coercivity H_C and the absolute SFD (σ_{SFD} , defined as the standard deviation σ of the Gaussian fitted to the derivative of the island reversal curve²) and normalized SFD (σ_{SFD}/H_C) versus pattern period. We observe a slight, nearly linear increase in the coercivity as we move to higher areal densities. This is expected for a well-behaved BPM system with little or no edge damage.⁷ The absolute and normalized SFDs increase as well with smaller pattern period.¹

The high anisotropy and coercivity of the $[\text{Co}(2.8 \text{ \AA})\text{Pd}(9 \text{ \AA})]_8$ ML are important to maintain thermal stability for densities $>1 \text{ Tb/in}^2$. However, higher write fields will be necessary in order to switch the islands. For recording applications the reversal fields of BPM need to be adjusted to match the field available from current write heads. One approach to lowering H_C of the Co/Pd ML system is reducing the ML anisotropy by increasing the individual Co layer thickness as shown in Fig. 2(a).^{10,12} The effects of increasing Co layer thickness while keeping the thickness integrated moment density $M_S \cdot t$ approximately

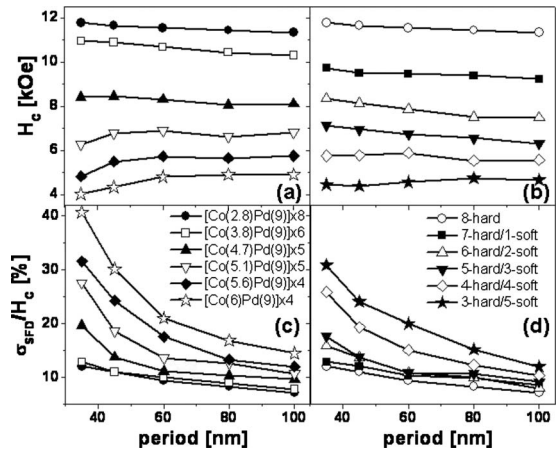


FIG. 3. Reduction in coercivity (H_C) and increase in normalized SFD (σ_{SFD}/H_C) for a series of Co/Pd ML films with increasing individual Co layer thickness [(a) and (c)] and for a series of laminated hard-soft Co/Pd-Co/Ni ML films with decreasing ratio of hard/soft number of repeats [(b) and (d)].

constant (by reducing the number of repeats) are shown in Fig. 3(a) and 3(c). Here H_C and σ_{SFD}/H_C are plotted as the individual Co thicknesses vary from 2.8 to 6 \AA causing H_C to decrease from 11 kOe down to 5 kOe .¹³ For higher anisotropy samples H_C keeps increasing slightly when reducing the island period as expected.¹ However, when the Co thickness exceeds about 5 \AA we observe a drop in H_C for densities above 180 Gb/in^2 (60 nm period) indicating that the perpendicular anisotropy of the ML film starts to degrade. At the same time the normalized SFD (σ_{SFD}/H_C) increases dramatically for Co thicknesses above 5 \AA confirming the assumption of a decrease in ML film quality.

A second approach for reducing H_C is the lamination of a hard ML with a relatively softer ML. In order to test this concept we use a $\text{Co}(2.8 \text{ \AA})/\text{Pd}(9 \text{ \AA})$ ML with $H_{K,\text{eff}}=21 \text{ kOe}$ and $M_S=500 \text{ emu/cm}^3$ as the hard layer and a $\text{Co}(1.5 \text{ \AA})/\text{Ni}(6 \text{ \AA})$ ML with $H_{K,\text{eff}}=5 \text{ kOe}$ and $M_S=700 \text{ emu/cm}^3$ as the soft layer. A corresponding sample series is shown in Figs. 3(b) and 3(d). Here we keep the total number of repeats constant ranging from 8 hard/0 soft repeats to 3 hard/5 soft repeats, thus covering the same coercivity range as before ($5\text{--}11 \text{ kOe}$).

Compared to the Co layer thickness series, this composite structure shows at higher areal densities a more consistent increase in H_C and also a less dramatic broadening of the normalized SFD. However, we still find a significant increase in normalized SFD as the soft layer thickness increases and becomes comparable to the hard layer thickness (4 hard/4 soft repeats). The thickness integrated moment density for both sample series was kept constant to within $\pm 10\%$ at $0.00043 \pm 0.00004 \text{ emu/cm}^2$, so that the dipolar interaction fields between the islands and the resulting dipolar broadening of the SFD are comparable.² Furthermore, samples of both series that match in coercivity also reveal a similar effective anisotropy $H_{K,\text{eff}}$ as shown in the inset of Fig. 4(a), which suggests comparable reversal modes for both sample series.¹⁴ Therefore the increase in measured SFD is due to an increase in the intrinsic SFD. All samples were prepared on identical pre-patterned substrates that were cut from a single wafer after patterning, such that overgrowth and edge effects are similar as well. Thus we hypothesize that the dominating factor causing an increase in the SFD is a change in the ML

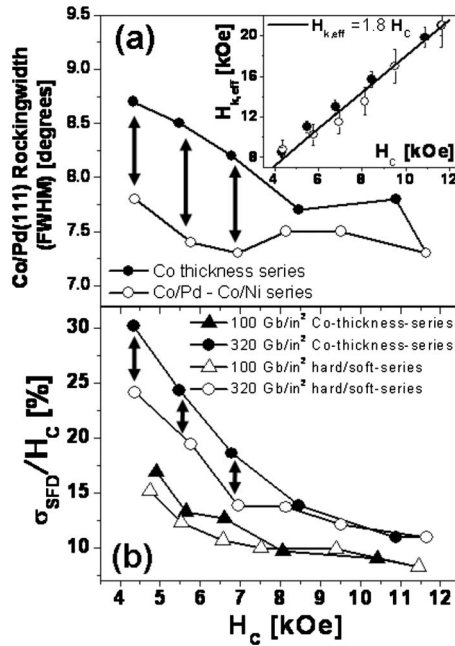


FIG. 4. (a) FWHM of the Co/Pd (111) out-of-plane directed crystallite distribution (mosaic spread) and (b) normalized SFD (σ_{SFD}/H_C) plotted versus coercive field (H_C) for both, the Co thickness and the Co/Pd (hard)—Co/Ni (soft) laminated sample series. The inset in (a) shows a plot of $H_{K,eff}$ vs H_C for both sample series.

film properties, such as interlayer roughness, strain, or crystallite size and orientation. X-ray reflectivity measurements show little interface roughness changes between samples, thus we focus on microstructure changes in the ML. For the high anisotropy reference sample we find a textured out-of-plane Co/Pd(111) mosaic spread with a FWHM of 7° – 7.5° . When increasing the Co thickness the mosaic spread also increases and reaches 8.7° for 6 \AA thick Co layers as shown in Fig. 4(a). In parallel we also observe an increase in the rocking-profile background intensity indicating that a small fraction of crystallites becomes completely misaligned with respect to the overall texture.¹⁵ For the laminated hard/soft sample series we do not see such changes in the crystallite distribution. Both sample series are compared in Fig. 4, where we plot the crystallite distribution for the full film samples versus the coercivity for the 320 Gb/in^2 patterns [Fig. 4(a)], together with the normalized SFD for the 100 and 320 Gb/in^2 patterns versus their respective coercivities [Fig. 4(b)]. The normalized SFD (σ_{SFD}/H_C) of the two series starts deviating from each other below about $H_C=8 \text{ kOe}$, which is consistent with the development of a difference in Co/Pd(111) out-of-plane crystallite alignment.

Additionally we measured the out-of-plane strain for the two sample series and found that the Co-thickness series also develops more strain than the hard/soft laminated structure. Thus both, a less ordered crystallite out-of-plane alignment and an increased strain may be the origin for the changes in SFD and the different H_C behavior for high areal densities in Fig. 3.^{3,15}

We also note that an improved SFD can arise if the Co/Pd and Co/Ni MLs are not fully correlated, i.e., if the value of the anisotropy of the Co/Ni component is not fully determined by the Co/Pd component on which it is deposited. In an uncorrelated system the normalized anisotropy distribution (and hence the SFD) can be reduced by a factor of up to $\sqrt{2}$ ^{16,17} due to the independent combination of the two sources of anisotropy within one island. This is in contrast to the homogeneous Co-thickness series where vertically we always have a fully correlated structure.

Overall our data and analysis suggests that it is favorable to use a laminated hard/soft layer approach in order to lower H_C in BPM based on Co/Pd ML systems. The laminated hard/soft system shows a more consistent coercivity versus areal density behavior (Fig. 3, top) and a smaller increase in normalized SFD (Fig. 3, bottom) for a coercivity range of 5 – 11 kOe . Possible reasons for this more favorable behavior of the hard-soft sample series are (1) the narrower c -axis distribution, (2) the more uncorrelated averaging over hard and soft layer SFDs in a laminated approach, and (3) some small exchange spring effect even though the soft layers are very thin and strongly exchange coupled to the hard layers.

¹T. Thomson, G. Hu, and B. D. Terris, *Phys. Rev. Lett.* **96**, 257204 (2006).

²O. Hellwig, A. Berger, T. Thomson, E. Dobisz, H. Yang, Z. Bandic, D. Kercher, and E. E. Fullerton, *Appl. Phys. Lett.* **90**, 162516 (2007).

³J. M. Shaw, W. H. Rippard, S. E. Russek, T. Reith, and C. M. Falco, *J. Appl. Phys.* **101**, 023909 (2007).

⁴M. S. Pierce, C. R. Buechler, L. B. Sorensen, J. J. Turner, S. D. Kevan, E. A. Jagla, J. M. Deutsch, T. Mai, K. Liu, J. H. Dunn, K. M. Chesnel, J. B. Kortright, O. Hellwig, and E. E. Fullerton, *Phys. Rev. Lett.* **94**, 017202 (2005).

⁵O. Hellwig, J. B. Kortright, A. Berger, and E. E. Fullerton, *J. Magn. Magn. Mater.* **319**, 13 (2007).

⁶M. E. Schabes, *J. Magn. Magn. Mater.* **320**, 2880 (2008).

⁷J. M. Shaw, S. E. Russek, T. Thomson, M. J. Donahue, B. D. Terris, O. Hellwig, E. Dobisz, and M. L. Schneider, *Phys. Rev. B* **78**, 024414 (2008).

⁸O. Hellwig, A. Moser, E. Dobisz, Z. Bandic, H. Yang, D. S. Kercher, J. D. Risner-Jamtegaard, D. Yaney, and E. E. Fullerton, *Appl. Phys. Lett.* **93**, 192501 (2008).

⁹J. Moritz, B. Dieny, J. P. Nozieres, S. Landis, A. Lebib, and Y. Chen, *J. Appl. Phys.* **91**, 7314 (2002).

¹⁰H. Nemoto and Y. Hosoe, *J. Appl. Phys.* **97**, 10J109 (2005).

¹¹V. Baltz, B. Rodmacq, A. Bollero, J. Ferré, S. Landis, and B. Dieny, *Appl. Phys. Lett.* **94**, 052503 (2009).

¹²B. Engel, C. D. England, R. A. Van Leeuwen, M. H. Wiedmann, and C. M. Falco, *Phys. Rev. Lett.* **67**, 1910 (1991).

¹³We note that we also observed a small decrease in anisotropy due to the change in the number of repeats from eight down to four, which may contribute some additional reduction to the reversal field.

¹⁴We note however that the hard/soft laminated sample series showed more curved hard axis hysteresis loops than the Co thickness series, thus suggesting some degree of exchange spring reversal mechanism for the hard/soft laminated structures.

¹⁵J. W. Lau, R. D. McMichael, S. H. Chung, J. O. Rantschler, V. Parekh, and D. Litvinov, *Appl. Phys. Lett.* **92**, 012506 (2008).

¹⁶ $\sigma_{total} = \sqrt{(\sigma_{hard} + c\sigma_{soft})^2} = \sqrt{\sigma_{hard}^2 + 2c\sigma_{hard}\sigma_{soft} + c^2\sigma_{soft}^2}$ where c is the correlation coefficient between the hard and the soft layer stack sigmas, with $c=0$ for totally uncorrelated hard and soft layer stacks and $c=1$ for totally correlated hard and soft layer stacks, thus if $\sigma_{hard} = \sigma_{soft} = \sigma$, then $\sigma_{total} = 2\sigma$ for $c=1$ and $\sigma_{total} = \sqrt{2}\sigma$ for $c=0$, which yields a difference of $\sqrt{2}$ in SFD for correlated versus uncorrelated hard and soft layer stacks.

¹⁷D. Suess, J. Lee, J. Fidler, and T. Schrefl, *J. Magn. Magn. Mater.* **321**, 545 (2009).